ICRP –1

DNA mutations and cancer

- Any mutation in a somatic cell (and particularly stem cells) can be step #1 toward cancer cell
- At least two mutations are needed to generate neoplastic phenotype and often more are needed.

Native DNA replication machinery is error prone

Table 1. Model parameters. These parameters were used for the algebraic model to see how colorectal cancer incidence scales with body size. Parameter values were taken from [7]. The mutation rate assumes that there are three genes (1 kb each) per pathway and a background mutation rate of 10^{-9} mutations per base pair per cell division.

parameter	value	definition
u	3×10^{-6}	mutations/oncogenic pathway/cell division
d	age(days)/4	divisions since birth (rate = 1 div./4 days)
k	6	rate liming mutations required for cancer
N	8	effective stem cells per crypt
m	$(1.5 \times 10^{-3} – 1.5 \times 10^{10})$	crypts per colon

F, Graham TA, Wang L-
CC. 2015 Solutions to
aradox revealed by
atical modelling and
ecies cancer gene
. Phil. Trans. R. Soc. B
.40222.

Native DNA replication machinery is error prone – evidence from increased numbers of new mutations in children as parents as they age

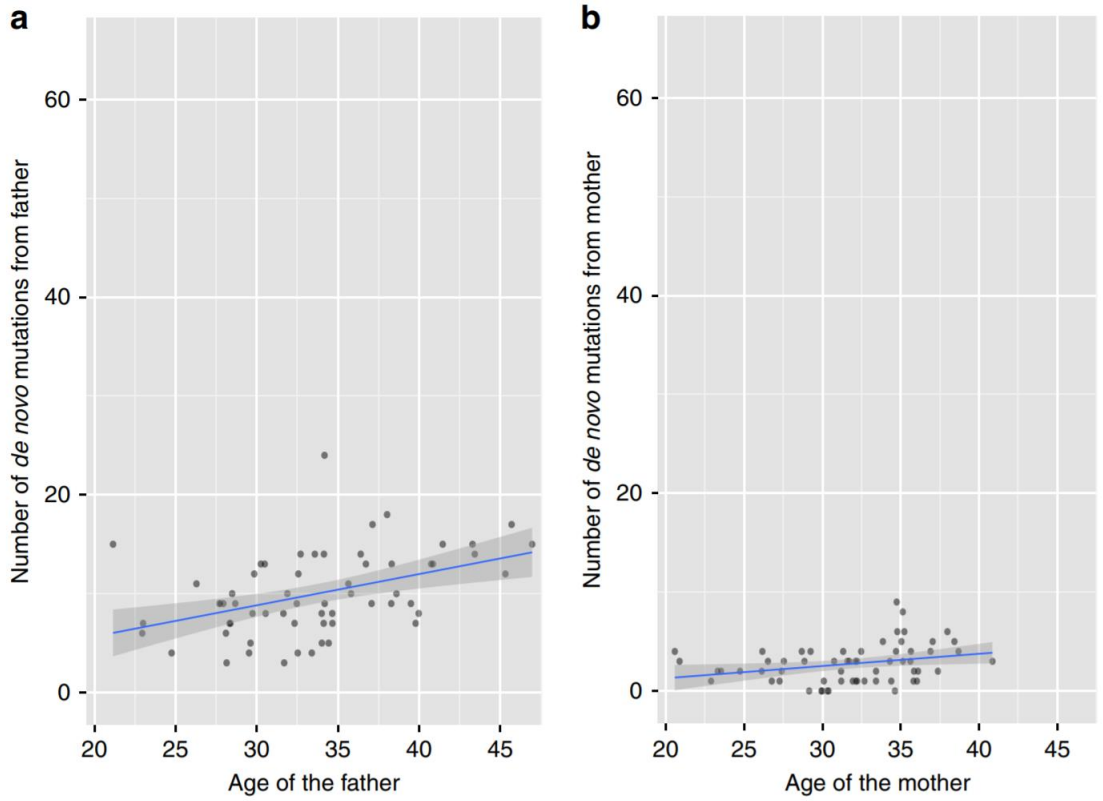

Figure 3 | Scatter plots with linear regression line on parental ages and their respective number of *de novo* mutations in the 61 trios with Illumina sequencing data. (**a**) The number of DNMs of paternal origin is plotted against the father's age (in years). The blue line shows the linear fit (estimate of the slope = 0.31, $P = 5.15 \times 10^{-4}$) and the grey band represents the 95% confidence interval. (**b**) The number of DNMs of maternal origin is plotted against the mother's age (in years), the blue line shows the linear fit (estimate of slope = 0.12, $P = 0.02$), and the grey band represents the 95% confidence interval.

Wendy S. W. Wong, Benjamin D. Solomon, Dale L. Bodian, Prachi Kothiyal, Greg Eley, Kathi C. Huddleston, Robin Baker, Dzung C. Thach, Ramaswamy K. Iyer, Joseph G. Vockley & John E. Niederhuber - Wong, W. S. W. et al. New observations on maternal age effect on germline de novo mutations. Nat. Commun. (2016).

Native DNA replication machinery is error prone – many cancers are spontaneous (at least initially)

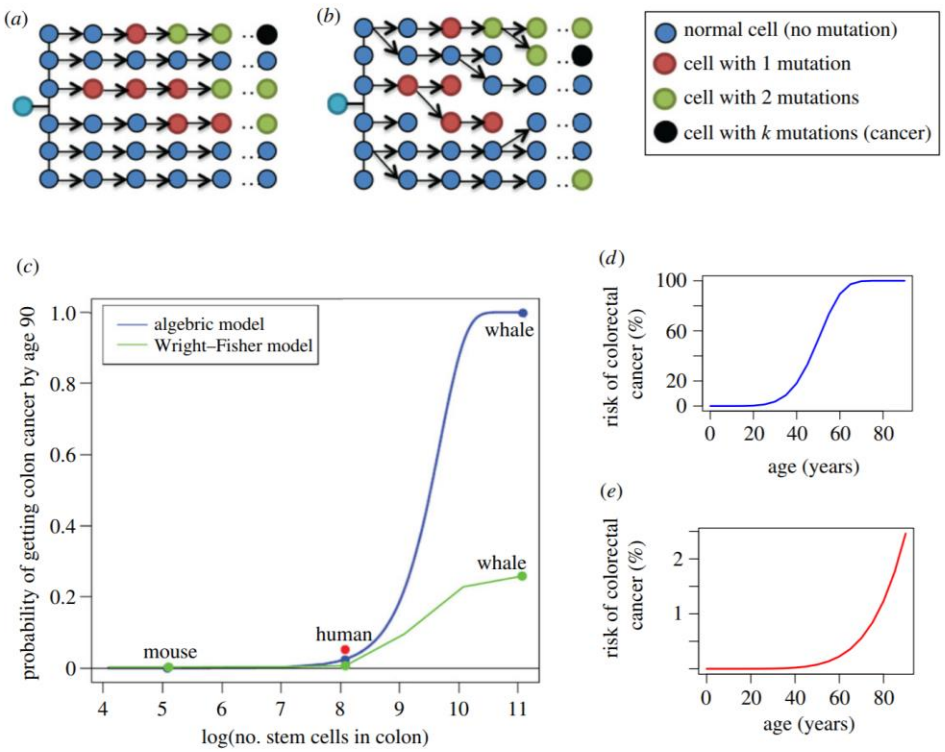

Figure 1. Estimated risk of colorectal cancer relative to body size under an algebraic and Wright–Fisher model. In the algebraic model (*a*) [7], cell lineages accumulate mutations over time, which are passed on to their daughter cell in the next generation and there is no cell death. In the Wright–Fisher model (*b*) [6], cells gain mutations over time, but each lineage has a chance of dying and being eliminated from the population. In both models, cancer occurs when a cell accumulates *k* mutations. The single light blue cell represents the zygote to show that all cells came from a single initial lineage. The probability was calculated using the algebraic and Wright–Fisher models with the parameters listed in table 1 [7] (*c*). Blue/green dots for mouse, human and whale indicate the estimated risk of colon cancer occurring within 90 years of life given the approximate number of cells in a human colon, 1000 times fewer cells to represent the mouse, and 1000 times more cells to represent the whale. The red dot indicates the lifetime risk of colon cancer according to the American Cancer Society which is about 5.3% for men and women averaged together [12]. The estimated age incidences of cancer for whale and human, given the algebraic model, are shown in (*d*) and (*e*), respectively. (*c–e*) Adapted from [2] with permission from Elsevier.

Caulin AF, Graham TA, Wang L-S, Maley CC. 2015 Solutions to Peto's paradox revealed by mathematical modelling and cross-species cancer gene analysis. Phil. Trans. R. Soc. B 370: 20140222.

Native DNA replication machinery AND numbers of stem cells may be inversely correlated to enable longevity

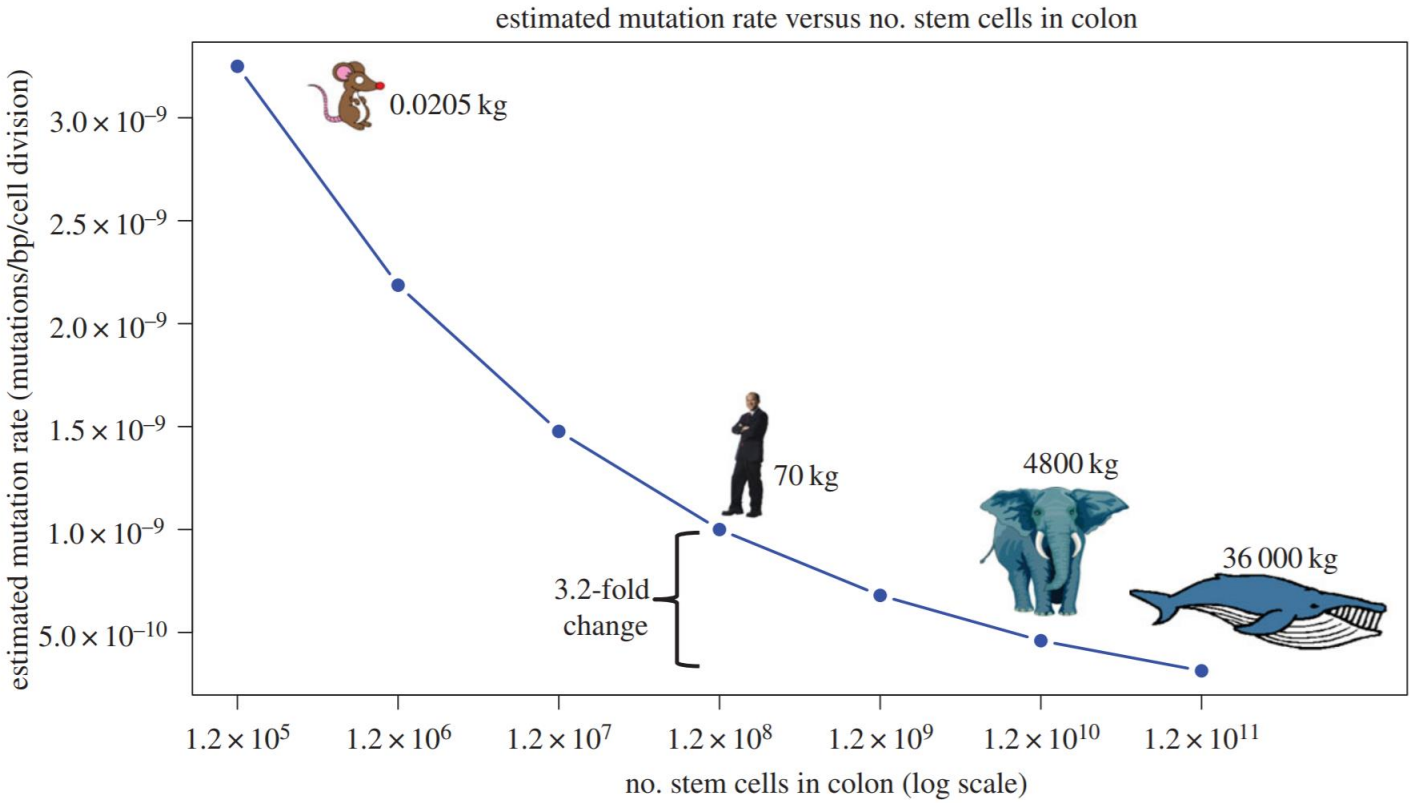

Figure 2. Estimated somatic mutation rates scaling with size. Mutation rate estimates show that a 3.2-fold decrease enables an animal that is 1000× larger (and so with 1000× more stem cells) than a human to have the same cancer risk. The mutation rates shown in the plot resulted in cancer risk predictions for the given number of cells that best matched the estimates for human (i.e. 1.2×10^8 colonic stem cells) using the Calabrese–Shibata algebraic model [7].

Caulin AF, Graham TA, Wang L-S, Maley CC. 2015 Solutions to Peto's paradox revealed by mathematical modelling and cross-species cancer gene analysis. Phil. Trans. R. Soc. B 370: 20140222.

Stem cells

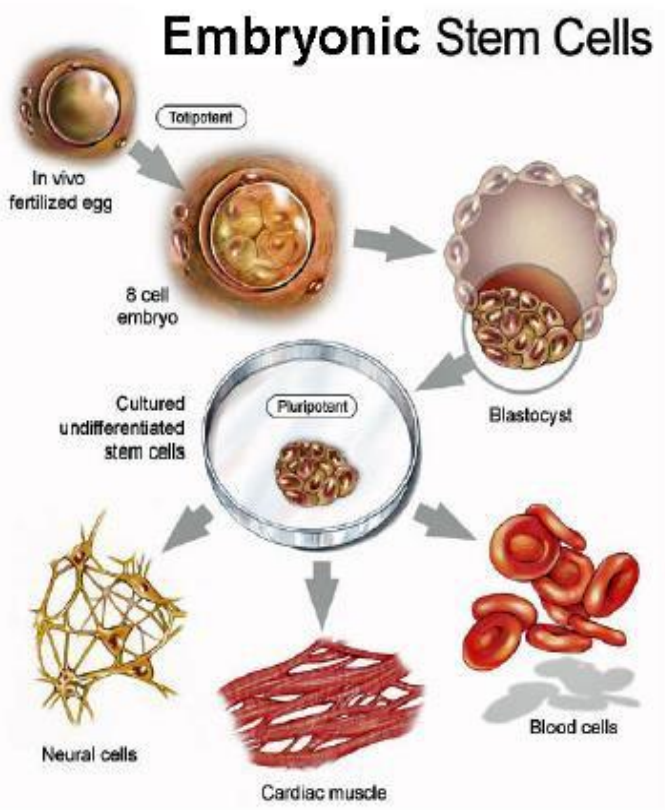

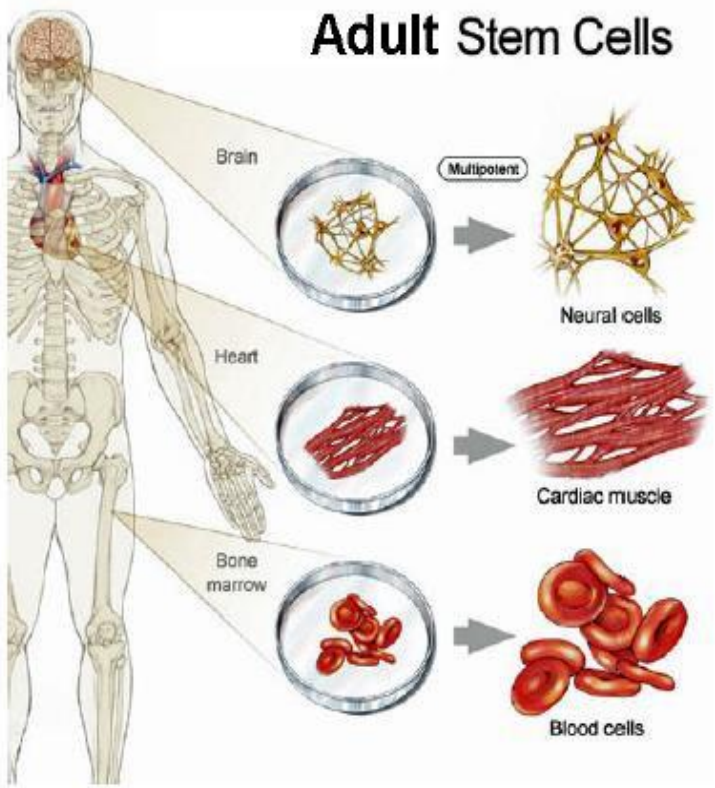

- Long-Term repopulating potential (LTRP)
- Self renewal
- Multi-lineage differentiation capacity

Cancer stem cells

- form in-vitro Sarcospheres
- highly tumorigenic after injection in recipient mice

(Red Fluorescence: Osteosarcoma cells were stabily labelled with Cherry-Fluorescence-Protein)

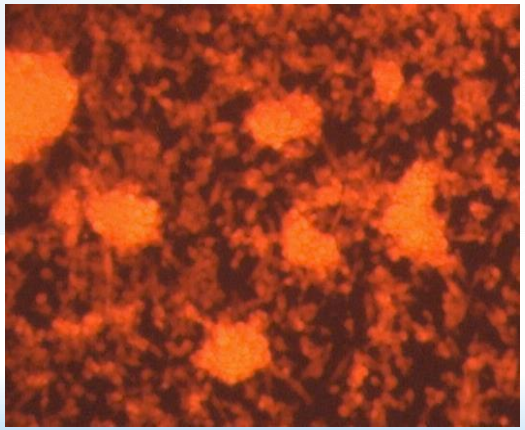

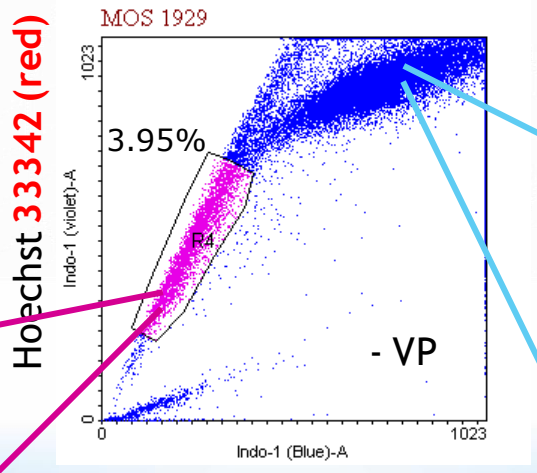

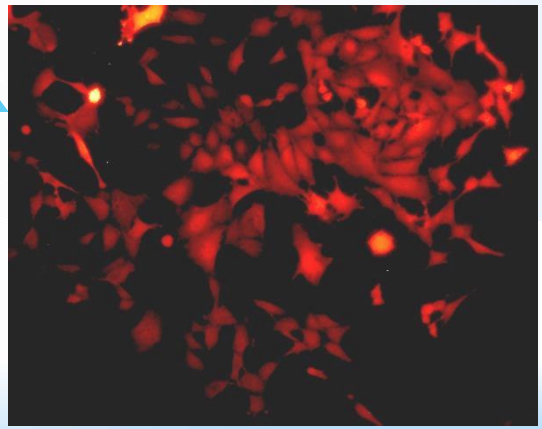

Multistep-Model of Carcinogenesis

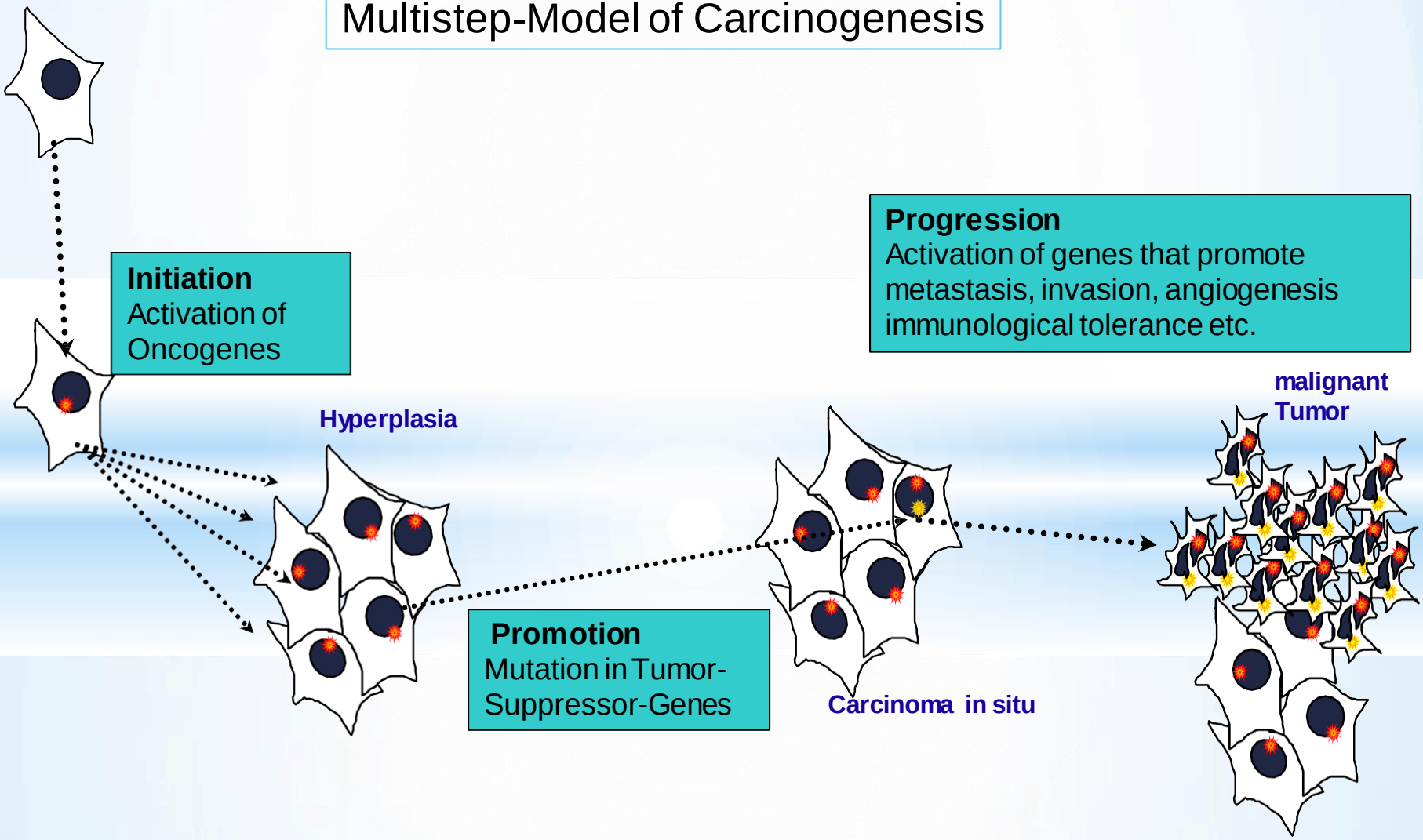

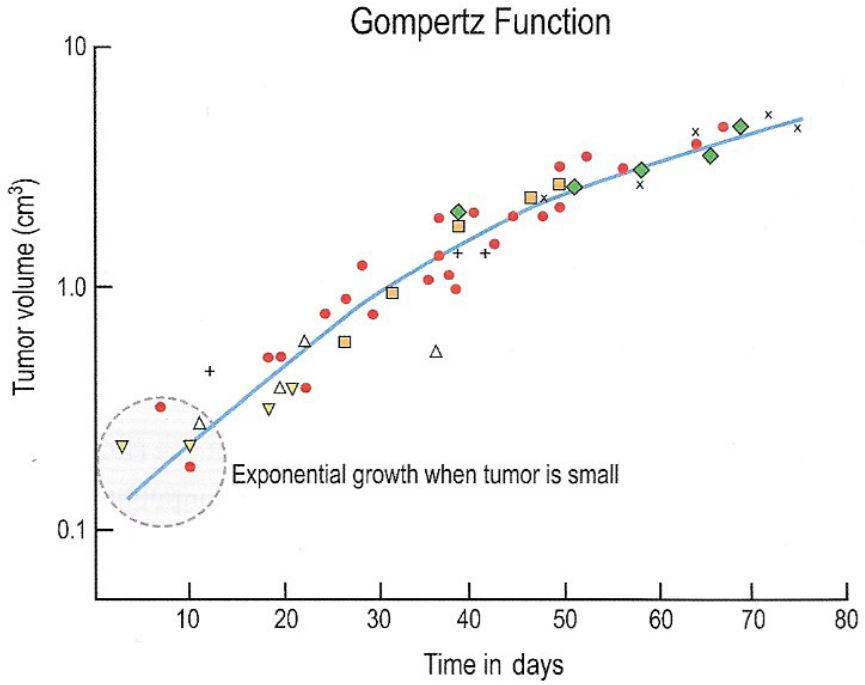

FIGURE 22.11 Illustrating a typical growth curve for an animal tumor, which is best fitted by a **Gompertz** function. When a tumor is composed of only a few cells, it may grow exponentially, but when it gets larger, the growth rate slows as the supply of oxygen and nutrients are outgrown.

E. J. Hall and A. J. Giaccia, "Radiobiology for the Radiologist," 8th Edition, Lippincott Williams & Wilkins, Philadelphia, 2018. pg. 411. Fig. 22.11

DNA mutations and radiation

- Ionizing radiation is one of possible sources of DNA mutations
- Ionizing radiation is considered a weak mutagen compared to many others
- At high enough doses, radiation can induce cell death as well

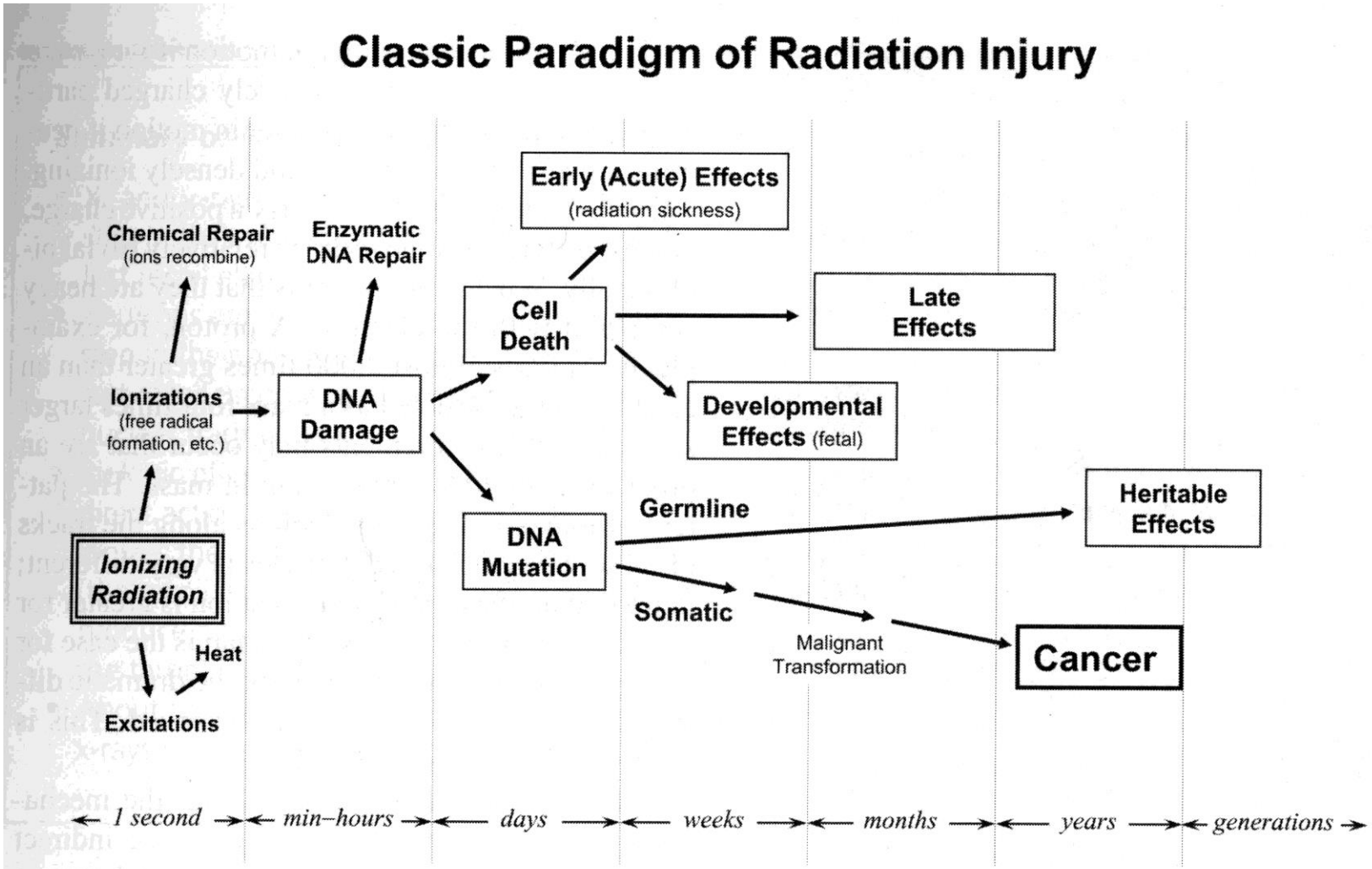

FIGURE 1.9 ● Illustration of the generally accepted sequence of events from the absorption of radation to the expression of the various forms of biological damage. (Developed in collaboration with Dr. Noelle Metting, U.S. Department of Energy.)

Ionizing Radiation
Dose Ranges
(Sievert)

acute exposure = all at once; chronic = hours, days, years

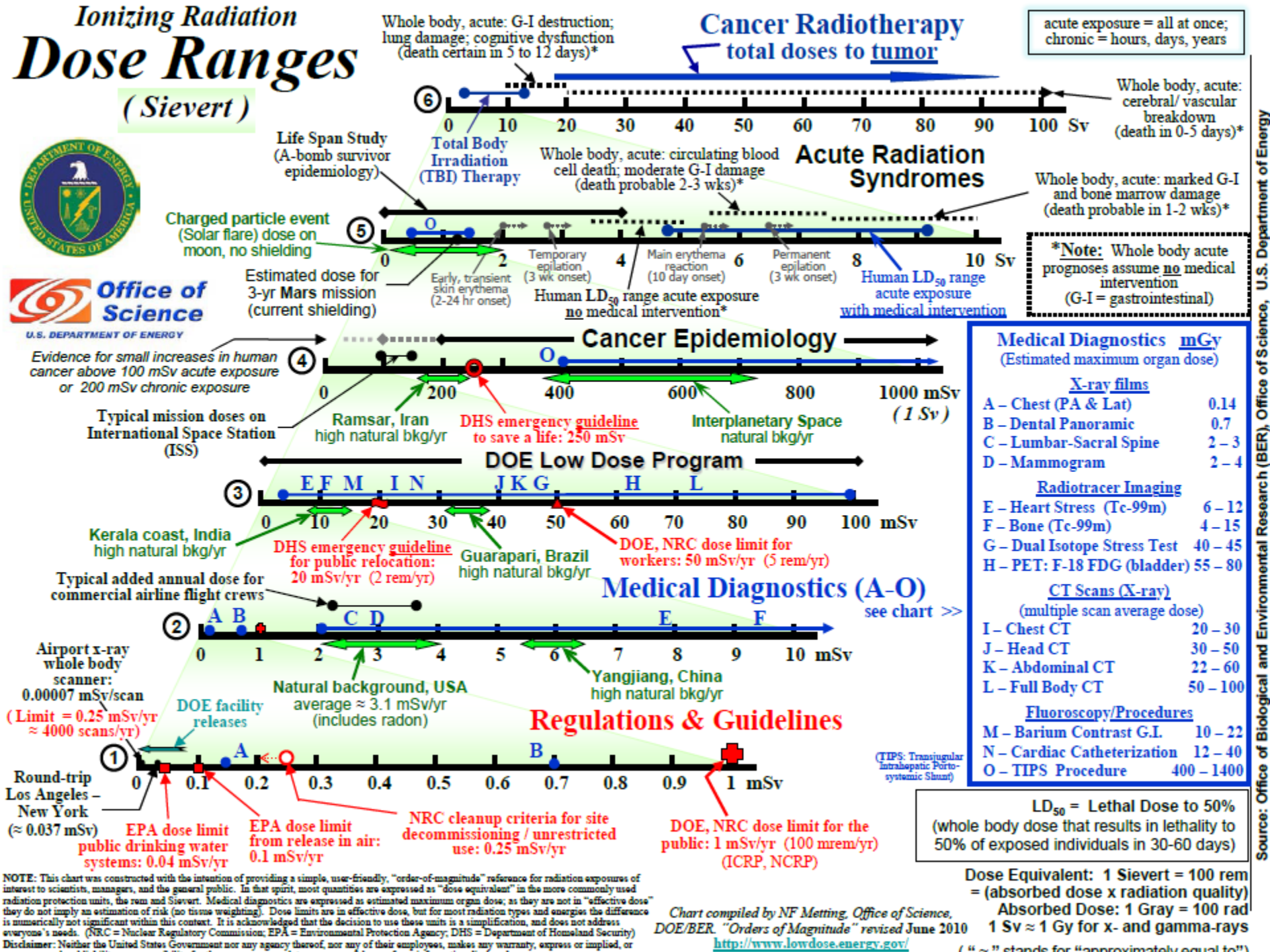

Medical Diagnostics mGy
(Estimated maximum organ dose)

X-ray films	
A – Chest (PA & Lat)	0.14
B – Dental Panoramic	0.7
C – Lumbar-Sacral Spine	2 – 3
D – Mammogram	2 – 4
Radiotracer Imaging	
E – Heart Stress (Tc-99m)	6 – 12
F – Bone (Tc-99m)	4 – 15
G – Dual Isotope Stress Test	40 – 45
H – PET: F-18 FDG (bladder)	55 – 80
CT Scans (X-ray) (multiple scan average dose)	
I – Chest CT	20 – 30
J – Head CT	30 – 50
K – Abdominal CT	22 – 60
L – Full Body CT	50 – 100
Fluoroscopy/Procedures	
M – Barium Contrast G.I.	10 – 22
N – Cardiac Catheterization	12 – 40
O – TIPS Procedure	400 – 1400

(TIPS: Transjugular Intrahepatic Porto-systemic Shunt)

LD_{50} = Lethal Dose to 50% (whole body dose that results in lethality to 50% of exposed individuals in 30-60 days)

Dose Equivalent: 1 Sievert = 100 rem = (absorbed dose x radiation quality)
Absorbed Dose: 1 Gray = 100 rad
1 Sv ≈ 1 Gy for x- and gamma-rays
(" ≈ " stands for "approximately equal to")

NOTE: This chart was constructed with the intention of providing a simple, user-friendly, "order-of-magnitude" reference for radiation exposures of interest to scientists, managers, and the general public. In that spirit, most quantities are expressed as "dose equivalent" in the more commonly used radiation protection units, the rem and Sievert. Medical diagnostics are expressed as estimated maximum organ dose; as they are not in "effective dose" they do not imply an estimation of risk (no tissue weighting). Dose limits are in effective dose, but for most radiation types and energies the difference is numerically not significant within this context. It is acknowledged that the decision to use these units is a simplification, and does not address everyone's needs. (NRC = Nuclear Regulatory Commission; EPA = Environmental Protection Agency; DHS = Department of Homeland Security)
Disclaimer: Neither the United States Government nor any agency thereof, nor any of their employees, makes any warranty, express or implied, or

Chart compiled by NF Metting, Office of Science, DOE/BER. "Orders of Magnitude" revised June 2010
http://www.lowdose.energy.gov/

Source: Office of Biological and Environmental Research (BER), Office of Science, U.S. Department of Energy

DNA and Ionizing Radiation

For Low LET radiation, 67% damage is indirect action

For High LET radiation, most (all?) damage is direct action

Critical distance of indirect IR action is within 2nm radius from DNA.

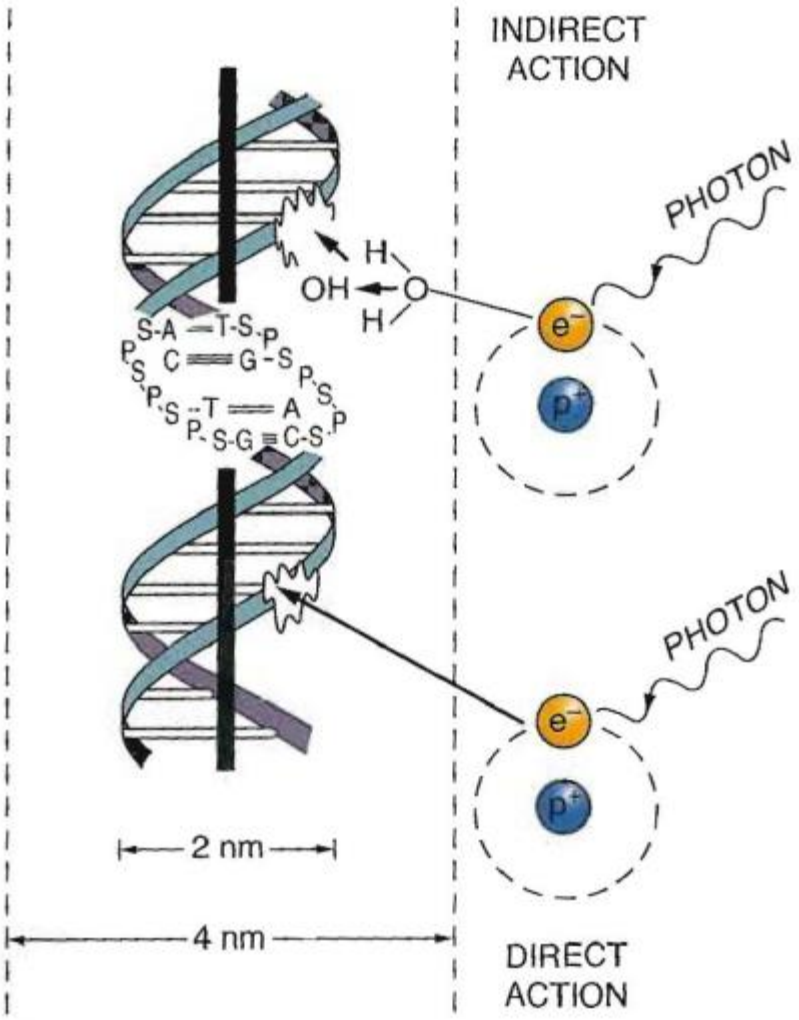

(From *Hall and Giaccia*)
Figure1.8 Direct and indirect actions of radiation.
The structure of DNA is shown schematically. In direct action, a secondary electron resulting from absorption of an x-ray photon interacts with the DNA to produce an effect. In indirect action, the secondary electron interacts with, for example,a water molecule to produce a hydroxyl radical (OH·), which in turn produces the damage to the DNA.The DNA helix has a diameter of about 20 A(2 nm). It is estimated that free radicals produced in a cylinder with a diameter double that of the DNA helix can affect the DNA. Indirect action is dominant for sparsely ionizing radiation, such as x-rays. S, sugar; P, phosphorus; A, adenine; T, thymine; G, guanine; C cytosine.

Low vs. High LET Ionization Pattern

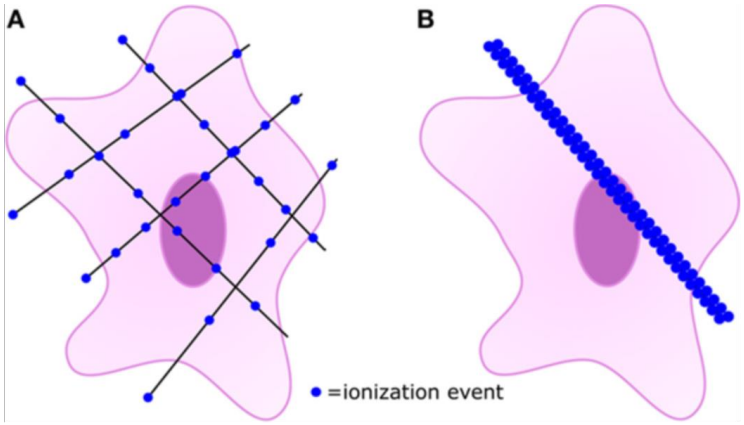

Sylvester CB, Abe JI, Patel ZS, Grande-Allen KJ. Radiation-Induced Cardiovascular Disease: Mechanisms and Importance of Linear Energy Transfer. Front Cardiovasc Med. 2018 Jan 31;5:5.

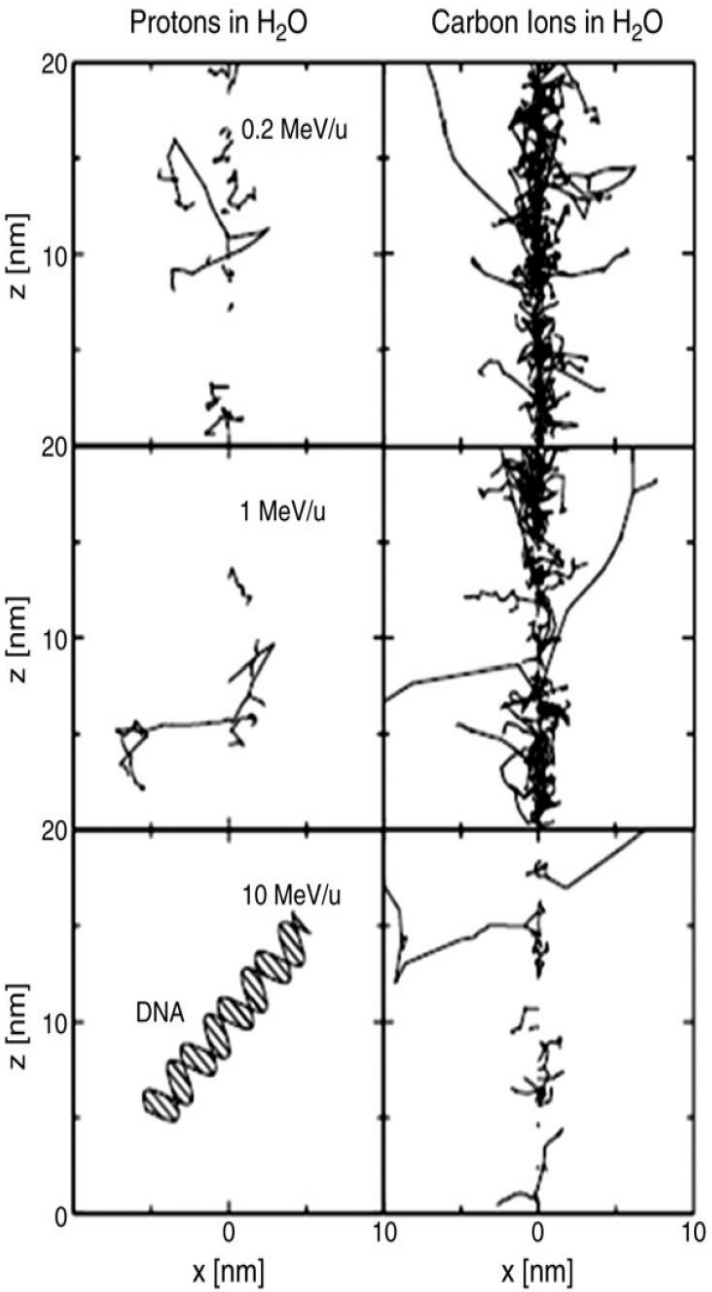

Proton and carbon ion tracks are compared microscopically to an illustration of a DNA molecule before, in and behind the Bragg maximum, for the same energy [41].

Fokas et al. Biochimica et Biophysica Acta 1796: 219

DNA Damage Induced by high and low LET

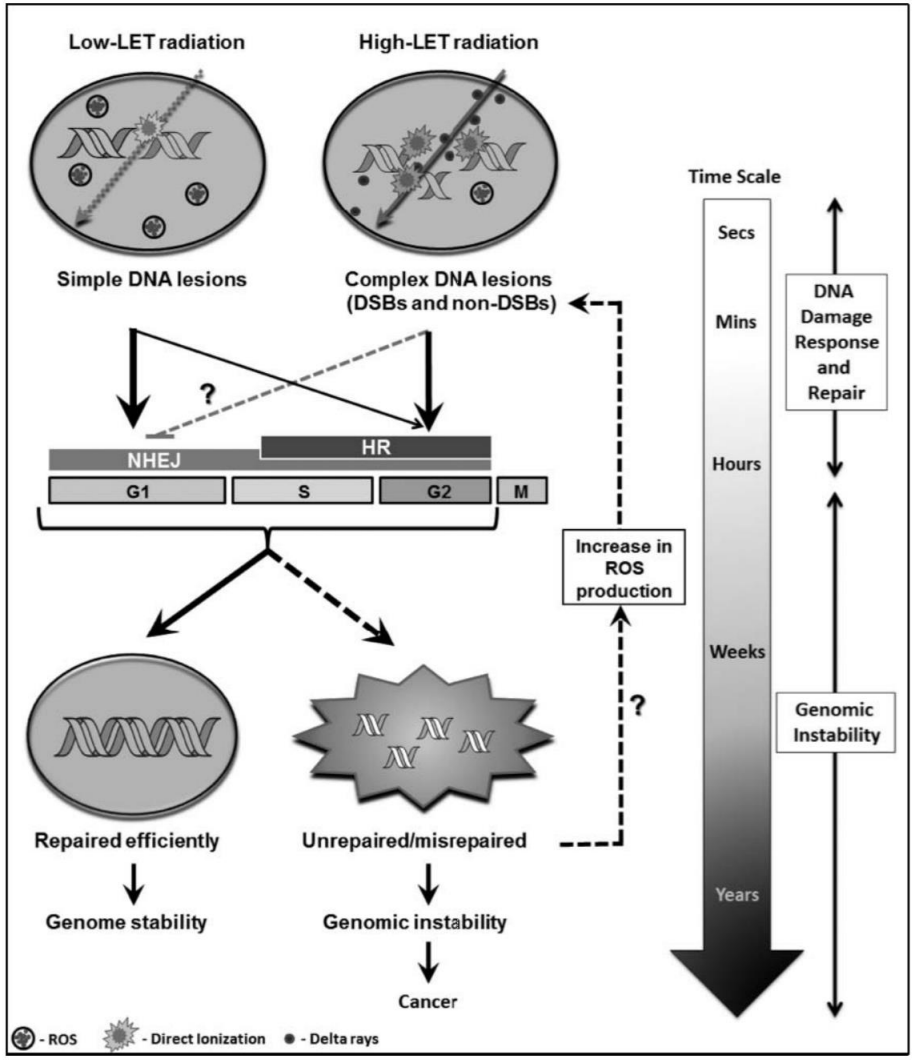

Repair of simple and complex DNA lesions induced by low- and high-LET radiation exposure. A majority of the DNA lesions induced by low-LET irradiation are simple lesions and are repaired within hours of induction via NHEJ- and HR-mediated repair pathways, with pathway preference dependent on cell cycle. On the other hand, a majority of the high-LET radiation-induced DNA damages are clustered lesions, which may impede DNA repair pathways, causing damage to remain unrepaired for longer periods (days to weeks). In addition to radiation-induced ROS, unrepaired DNA lesions may also increase the ROS levels in cells, causing further generation of simple to complex DNA lesions. Unrepaired/misrepaired lesions in mitochondrial or nuclear DNA (dotted line) may also further enhance and perpetuate ROS levels. Ultimately, the unrepaired/ misrepaired DNA lesions may promote genomic instability, leading to initiation of carcinogenesis

Sridharan, D. M., Asaithamby, A., Bailey, S. M., Costes, S., Doetsch, P. W., Dynan, W., Kronenberg, A., Rithidech, K. N., Saha, J., Snijders, A. M., Werner, E., Wiese, C., Cucinotta, F. A. and Pluth, J. M. Understanding Cancer Development Processes after HZE-Particle Exposure: Roles of ROS, DNA Damage Repair, and Inflammation. Radiat. Res. 183, 1–26 (2015).

RBE vs. LET

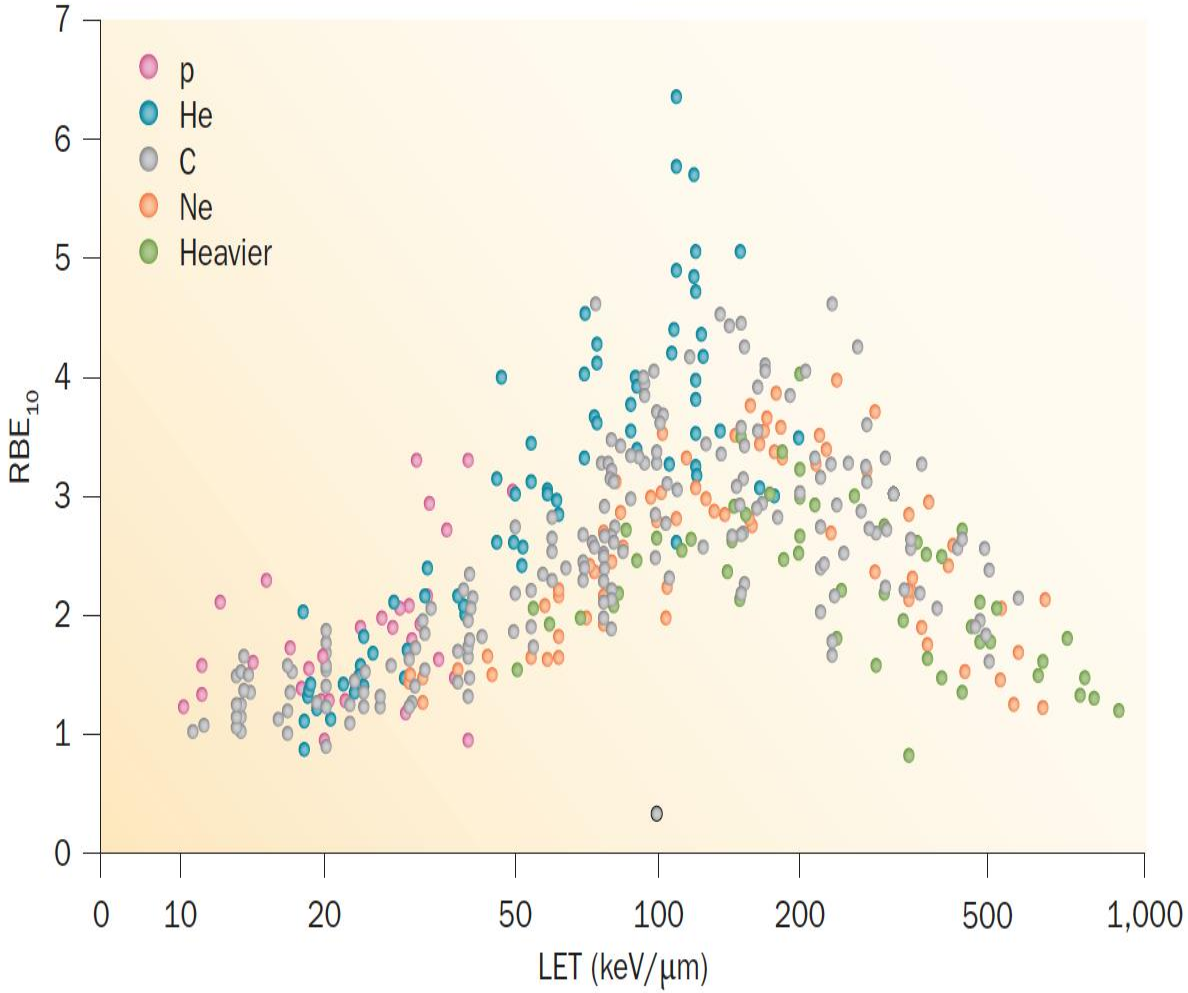

RBE versus LET from published experiments on in vitro cell lines. RBE is calculated at 10% survival, LET values are given is keV/µm in water. Different colours indicate different ions, from protons to heavy ions. Data points are extracted from the Particle Radiation Data Ensemble (PIDE) database,162 which currently includes 855 survival curves for cells exposed to photons (α/β ratio ranging 1–30) and ions. Abbreviations: LET, linear energy transfer; RBE, relative biological effectiveness.

Loeffler and Durante, Nat Rev Clin Oncol. 2013 10(7):411-24.

Cell and Tissue Damage

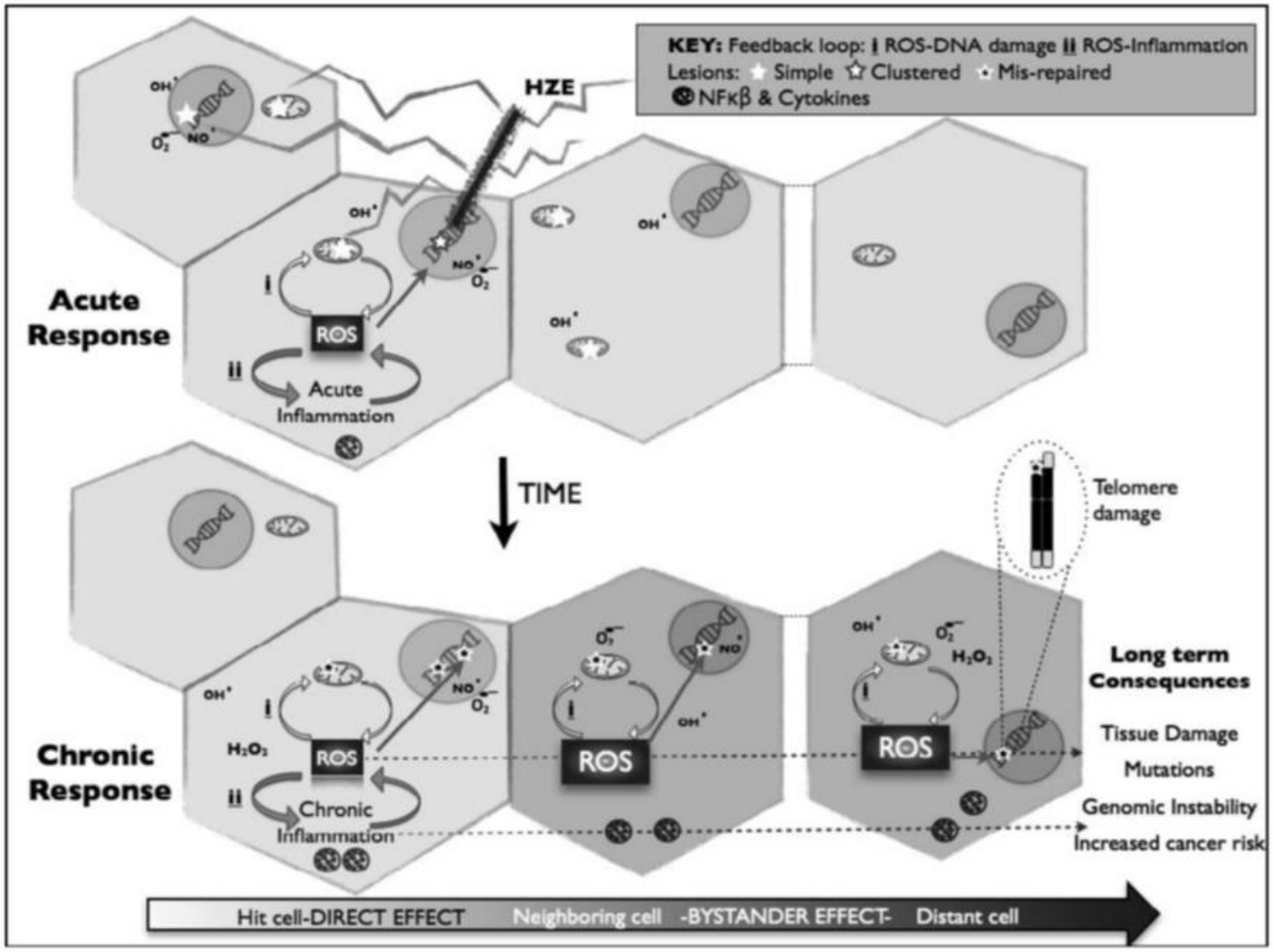

Sridharan, D. M., Asaithamby, A., Bailey, S. M., Costes, S., Doetsch, P. W., Dynan, W., Kronenberg, A., Rithidech, K. N., Saha, J., Snijders, A. M., Werner, E., Wiese, C., Cucinotta, F. A. and Pluth, J. M. Understanding Cancer Development Processes after HZE-Particle Exposure: Roles of ROS, DNA Damage Repair, and Inflammation. Radiat. Res. 183, 1–26 (2015).

Schematic representation of known mechanistic links between biomarkers that define cell fates, which promote or protect from cancer risk

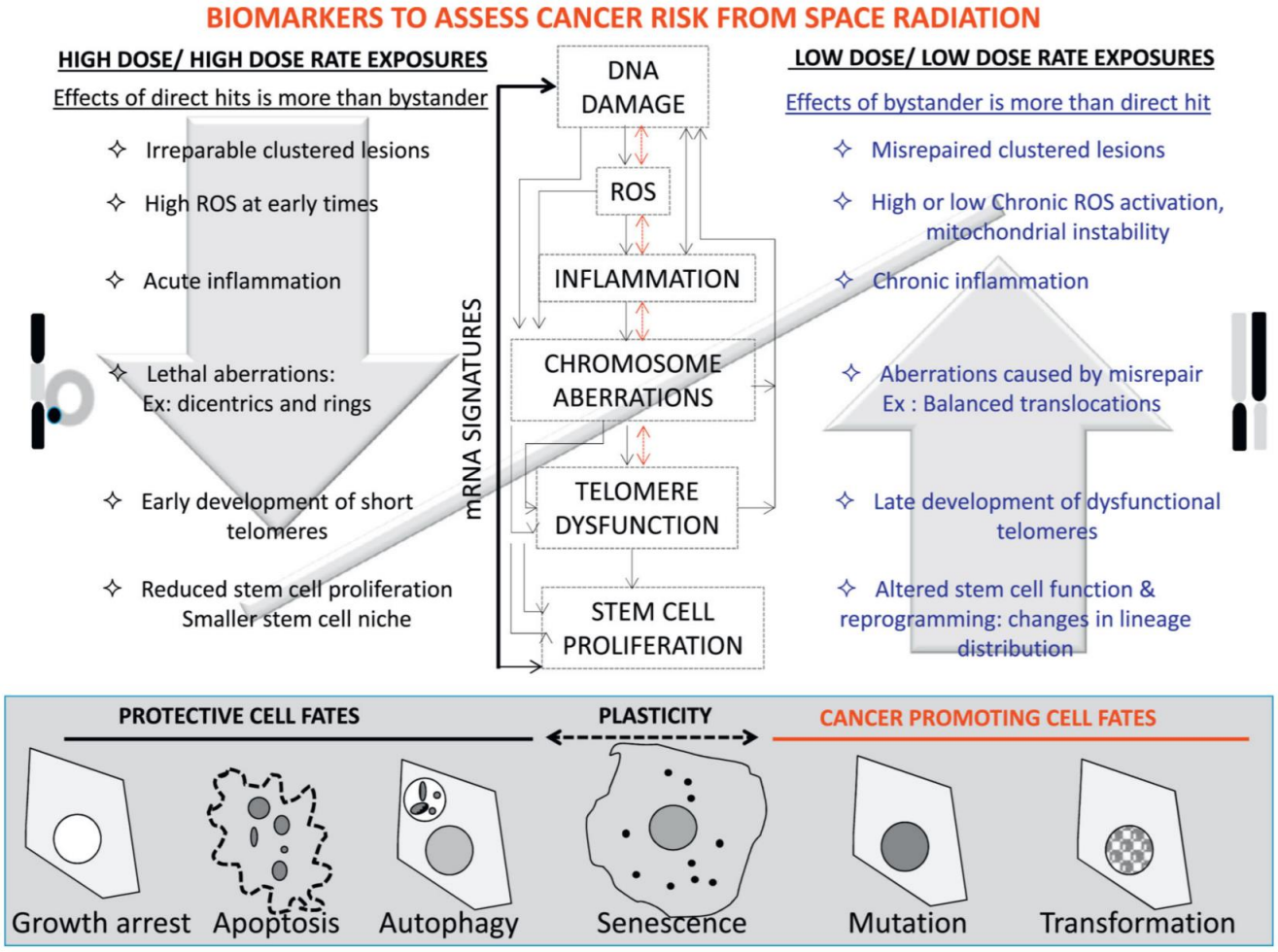

Sridharan DM, Asaithamby A, Blattnig SR, Costes SV, Doetsch PW, Dynan WS, Hahnfeldt P, Hlatky L, Kidane Y, Kronenberg A, Naidu MD, Peterson LE, Plante I, Ponomarev AL, Saha J, Snijders AM, Srinivasan K, Tang J, Werner E, Pluth JM. Evaluating biomarkers to model cancer risk post cosmic ray exposure. Life Sci Space Res (Amst). 2016 Jun;9:19-47.

Sources of Ionizing Radiation

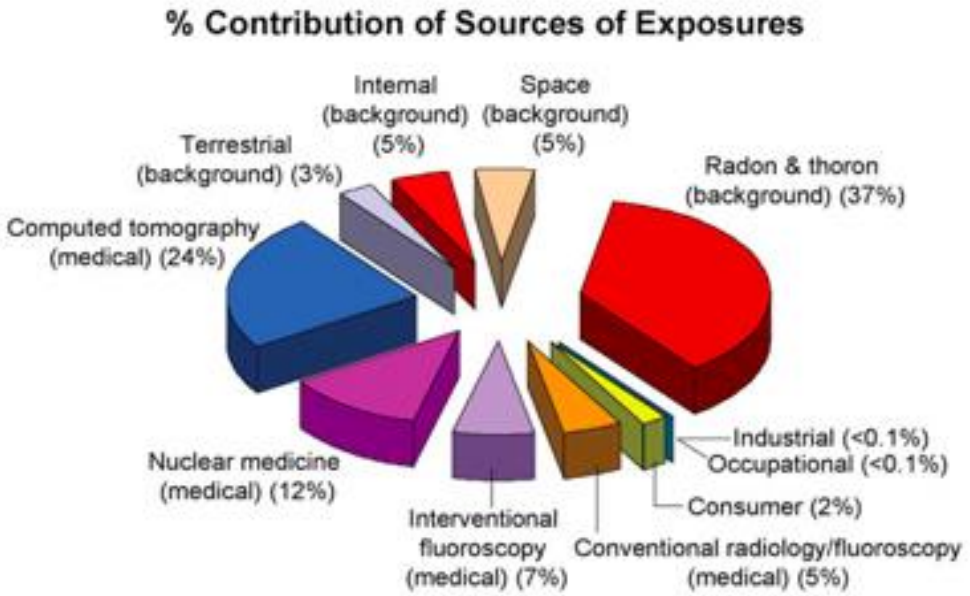

FIGURE 16.6 Percentage contribution of the various sources of exposure to the collective effective dose (1,870,000 person-Sv) and the average total effective dose per person in the US population (6.2 mSv) for 2006. Medical radiation and natural background radiation make almost equal contributions. (Data from National Council on Radiation Protection and Measurements. *Ionizing Radiation Exposure of the Population of the United States. Report 160.* Bethesda, MD: NCRP; 2009.)

Hall 2012 figure 16.6

Annual risk (Americans, excluding radiation therapy)

- Radon, 'natural', but preventable, causes ~10% of all lung cancer, according to BEIR VI
- Medical imaging procedures contribute almost 50% of total exposure, which would contribute ~ 50K fatal cancers, however much of this is delivered to fatally ill patients.
- Occupational exposure only causes ~100 cancers per year, but this is concentrated in a small cohort -- consisting mostly of aviation and medical workers.

Sources of Ionizing Radiation

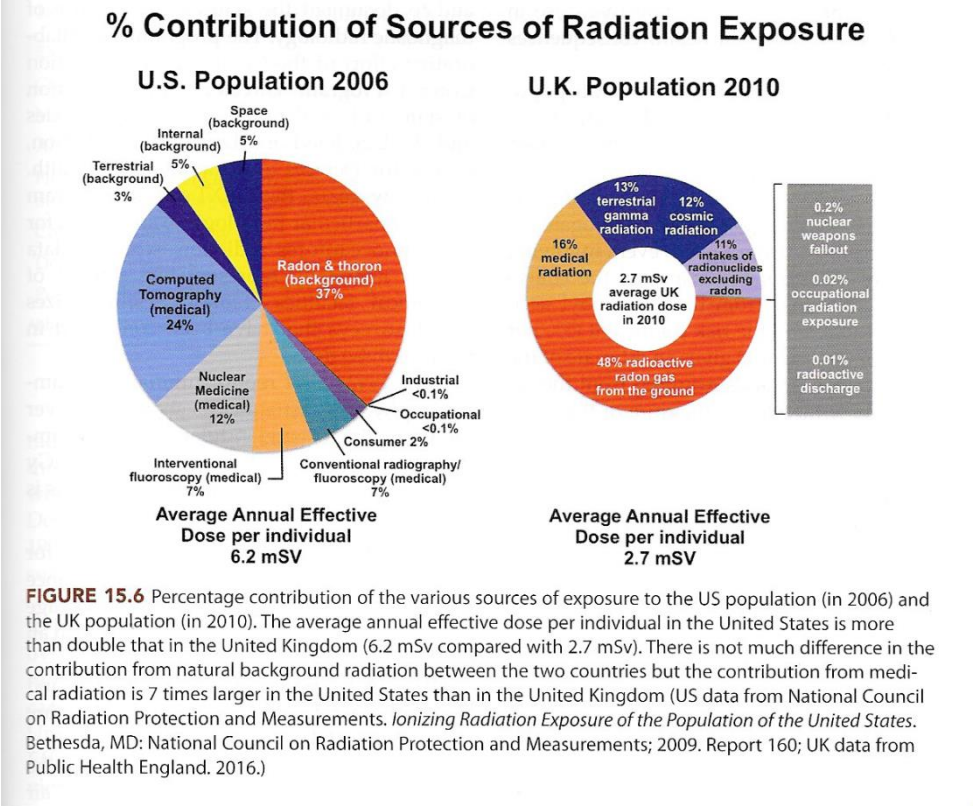

FIGURE 15.6 Percentage contribution of the various sources of exposure to the US population (in 2006) and the UK population (in 2010). The average annual effective dose per individual in the United States is more than double that in the United Kingdom (6.2 mSv compared with 2.7 mSv). There is not much difference in the contribution from natural background radiation between the two countries but the contribution from medical radiation is 7 times larger in the United States than in the United Kingdom (US data from National Council on Radiation Protection and Measurements. *Ionizing Radiation Exposure of the Population of the United States*. Bethesda, MD: National Council on Radiation Protection and Measurements; 2009. Report 160; UK data from Public Health England. 2016.)

E. J. Hall and A. J. Giaccia, "Radiobiology for the Radiologist," 8th Edition, Lippincott Williams & Wilkins, Philadelphia, 2018. pg. 211. Fig. 15.6

Exceptional acute and chronic radiation exposures

Acute radiation effects at high doses are separated into distinct syndromes

FIGURE 9.2 Showing the result of an experiment in which nonhuman primates were given the granulocyte colony-stimulating factor (G-CSF, filgrastim [Neupogen]) 24 hours after a total-body irradiation (TBI) of 7.5 Gy. Eighty percent of the animals survived compared with 40% in controls that did not receive the G-CSF. In other experiments (results not shown), the agent proved to be ineffective if administration was delayed to 48 hours postirradiation. (Adapted from Farese AM, Cohen MV, Katz BP, et al. Filgrastim improves survival in lethally irradiated nonhuman primates. *Radiat Res.* 2013;179:89–100; and Farese AM, Brown CR, Smith CP, et al. The ability of filgrastim to mitigate mortality following $LD_{50/60}$ total-body irradiation is administration time-dependent. *Health Phys.* 2014;106[1]:39–47.)

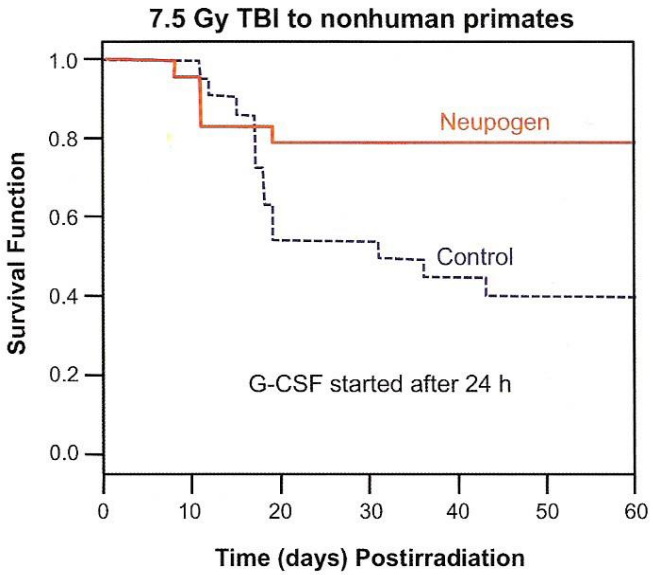

E. J. Hall and A. J. Giaccia, "Radiobiology for the Radiologist," 8th Edition, Lippincott Williams & Wilkins, Philadelphia, 2018. pg. 130, Fig 9.2

Post radiation events include different types of cancer– numbers of stem cells affected are important when cancer type is to be considered

FIGURE 10.17 Relative risk of leukemia, excluding chronic lymphocytic leukemia, associated with 2-year lagged cumulative red bone marrow dose. The *lines* are the fitted linear dose–response model for different dose ranges, whereas the *shaded areas* represent the 90% CIs. (Adapted from Leuraud K, Richardson DB, Cardis E, et al. Ionising radiation and risk of death from leukaemia and lymphoma in radiation-monitored workers [INWORKS]: an international cohort study. *Lancet Haematol.* 2015;2:e276–e281.)

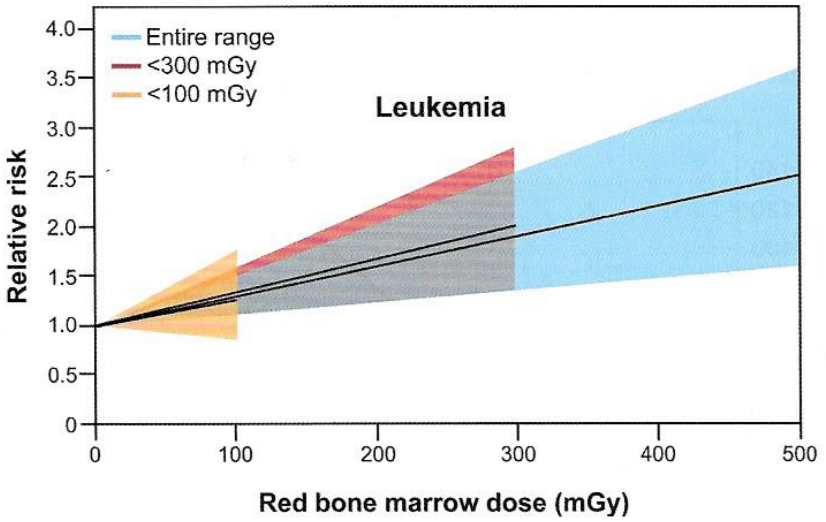

E. J. Hall and A. J. Giaccia, "Radiobiology for the Radiologist," 8th Edition, Lippincott Williams & Wilkins, Philadelphia, 2018. pg. 154 Fig. 10.17

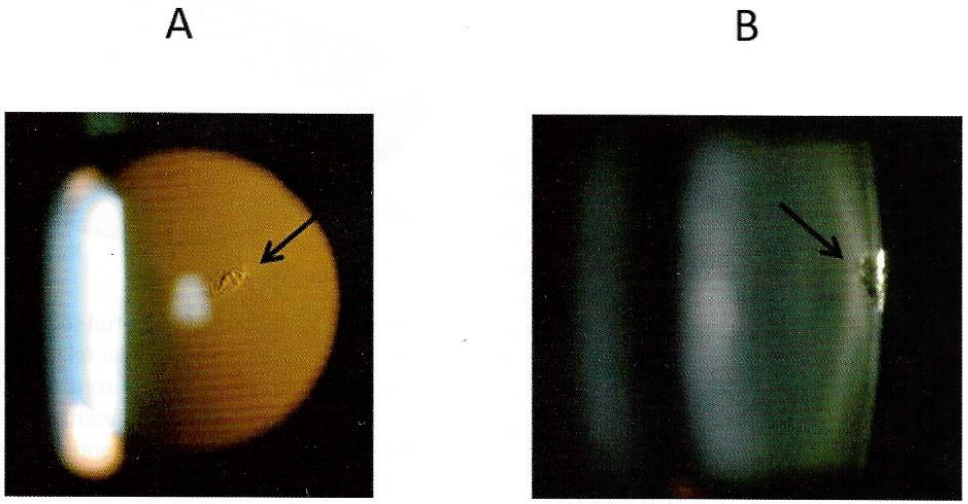

FIGURE 13.2 Clinical appearance of a typical radiation cataract in the posterior scapular region in an interventional cardiologist with 22 years of occupational radiation exposure. **A:** Retroillumination image (i.e., using the light that is reflected by the retina back through the lens). **B:** Conventional slit lamp imaging (i.e., where an optical section of the lens is directly visualized). In both cases, the position of the opacity is indicated by an arrow. (Courtesy of Dr. Norman Kleiman.)

E. J. Hall and A. J. Giaccia, "Radiobiology for the Radiologist," 8th Edition, Lippincott Williams & Wilkins, Philadelphia, 2018. pg. 192. Fig. 13.2

Radiation uses in therapy

- High doses – low volume of tissue

Radiation and dual checkpoint blockade activate non-redundant immune mechanisms in cancer

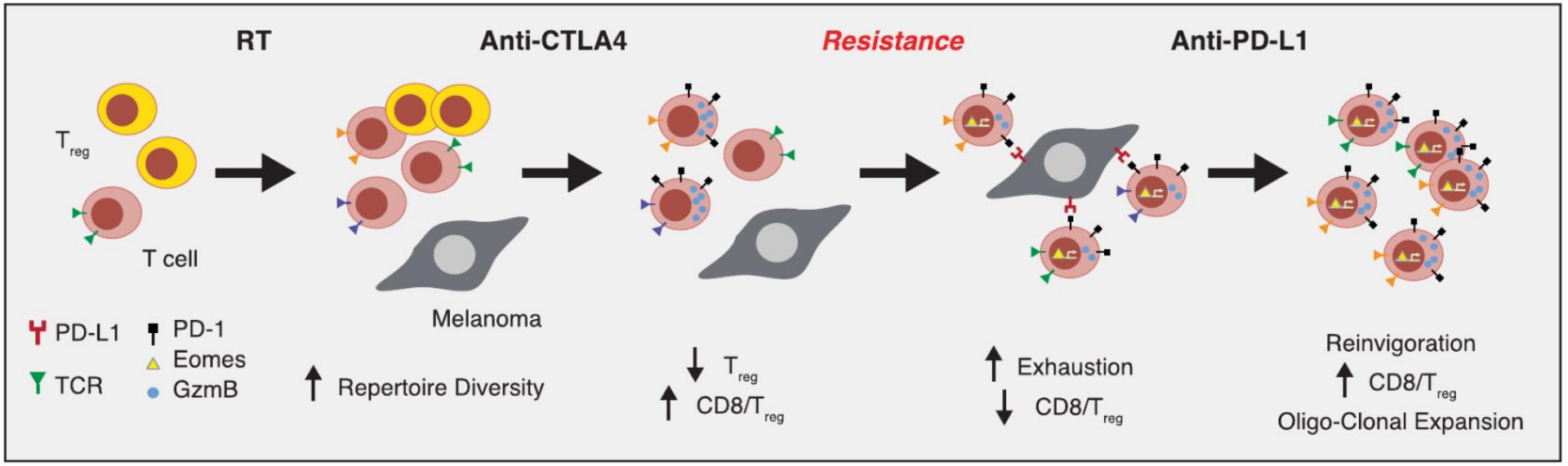

Model for non-redundant mechanisms and resistance to RT and immune checkpoint blockade.

Twyman-Saint Victor et al., Nature. 2015 Apr 16;520(7547):373-7.

Radiation and immunotherapy against cancer are not often mentioned from the immune system perspective

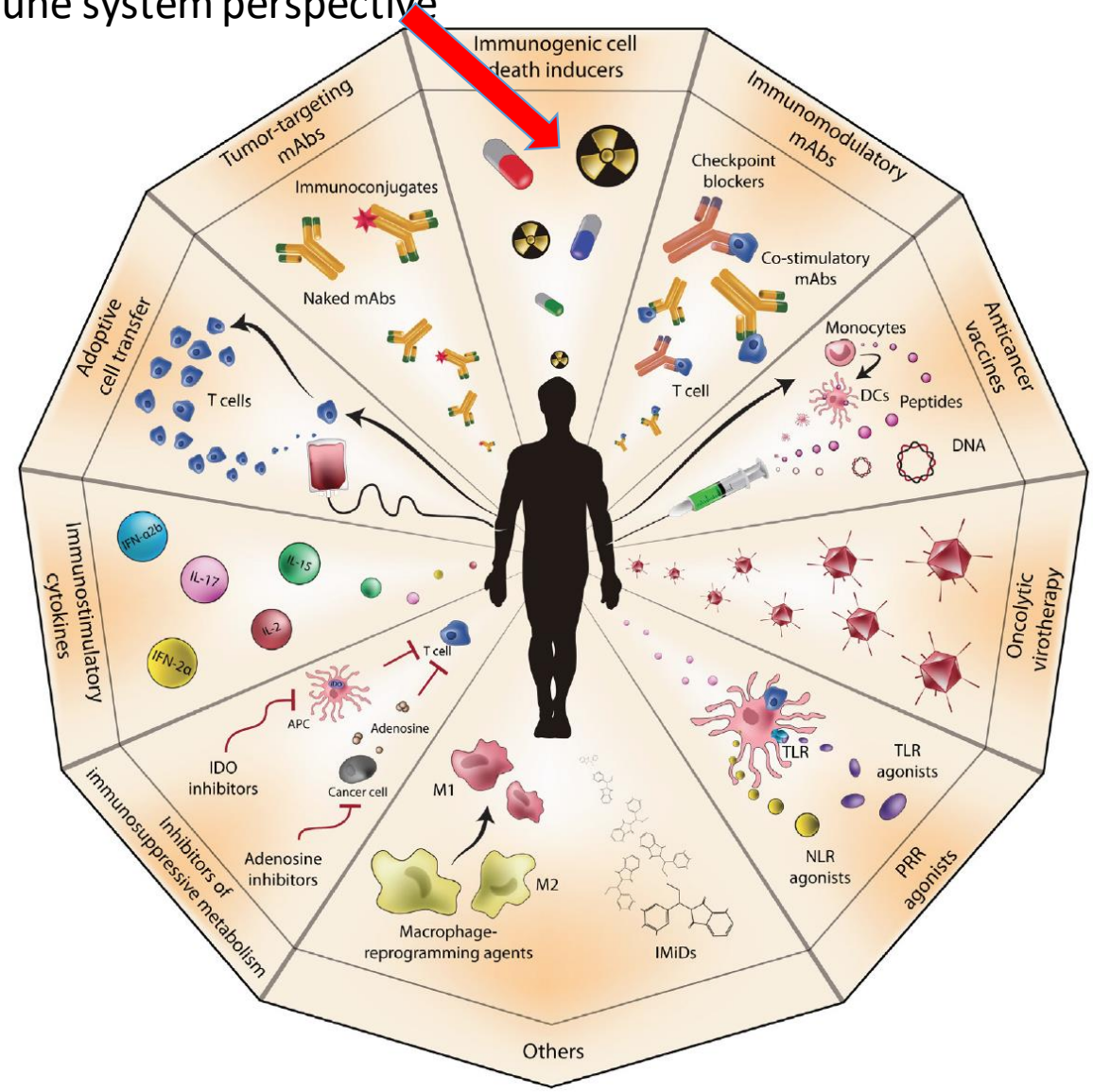

Anticancer immunotherapy. Several anticancer immunotherapeutics have been developed during the last three decades, including tumor-targeting and immunomodulatory monoclonal antibodies (mAbs); dendritic cell (DC)-, peptide- and DNA-based anticancer vaccines; oncolytic viruses; pattern recognition receptor (PRR) agonists; immunostimulatory cytokines; immunogenic cell death inducers; inhibitors of immunosuppressive metabolism; and adoptive cell transfer. 1MT, 1-methyltryptophan; APC, antigen-presenting cell; IDO, indoleamine 2,3-dioxigenase; IFN, interferon; IL, interleukin; IMiD, immunomodulatory drug; NLR, NOD-like receptor; TLR, Toll-like receptor.

Galluzzi et al., Classification of current anticancer immunotherapies. Oncotarget. 2014 Dec 30;5(24):12472-508.

Combinations of immunotherapy and radiation in cancer therapy

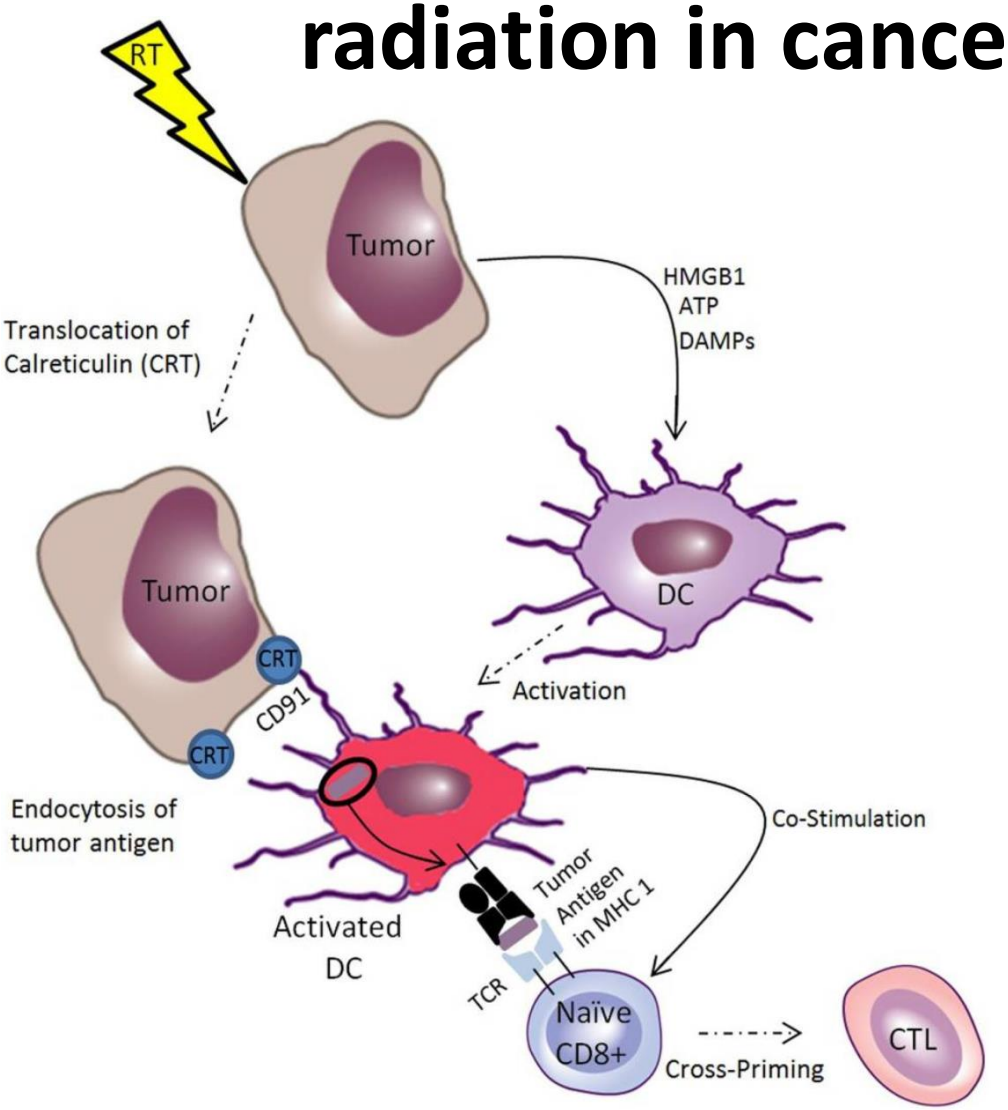

Ionizing radiation induces immunogenic cell death of tumors, which facilitates cross-priming of CTLs. Ionizing radiation induces translocation of calreticulin (CRT) to the tumor cell membrane, which acts as an "eat me" signal to dendritic cells (DCs), facilitating receptor mediated endocytosis through CD91. This makes tumor antigens available for cross-presentation on MHC-I for priming of tumor-specific T-cells. Radiotherapy also induces the release of danger associated molecular patterns (DAMPs), such as ATP and HMGB-1, which are endogenous immune adjuvants that stimulate DC activation, inducing DCs to provide co-stimulatory signals to naïve T-cells, facilitating cross-priming of CTLs. Together, these processes constitute immunogenic cell death of tumor cells.

Vatner RE, Cooper BT, Vanpouille-Box C, Demaria S, Formenti SC. Combinations of immunotherapy and radiation in cancer therapy. Front Oncol. 2014 Nov 28;4:325. PMCID: PMC4246656.

LNT model … or not

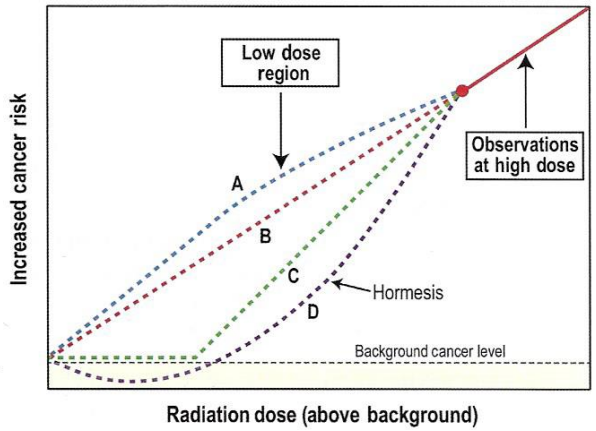

FIGURE 10.19 Illustrating the controversy of how to extrapolate cancer risks from high doses, for which there are epidemiologic data, to low doses characteristic of the radiation protection scenario. *Line B* illustrates the linear no–threshold hypothesis, favored by BEIR, UNSCEAR, ICRP, and NCRP. *Line A* assumes that risks are higher at low doses than would be predicted from a linear extrapolation. This might, for example, be a consequence of the bystander effect. *Line C* assumes that there is a threshold in dose, below which there are no deleterious biologic effects. *Line D* illustrates the hypothesis that low levels of radiation are beneficial, activating repair mechanisms that protect against disease; this is known as *hormesis*.

E. J. Hall and A. J. Giaccia, "Radiobiology for the Radiologist," 8th Edition, Lippincott Williams & Wilkins, Philadelphia, 2018. pg. 155. Fig 10.19